Carbohydrate Polymers 90 (2012) 1371–1377

Contents lists available at SciVerse ScienceDirect

Carbohydrate Polymers

journal homepage: www.elsevier.com/locate/carbpol

Self-assembly of amylose-grafted carboxymethyl cellulose

Jun-ichi Kadokawa*, Takuya Arimura, Yasutaka Takemoto, Kazuya Yamamoto

Graduate School of Science and Engineering, Kagoshima University, 1-21-40 Korimoto, Kagoshima 890-0065, Japan

ARTICLE INFO

Article history:
Received 15 May 2012
Received in revised form 23 June 2012
Accepted 2 July 2012
Available online 10 July 2012

Keywords:
Amylose
Carboxymethyl cellulose
Chemoenzymatic
Nanofiber
Self-assembly

ABSTRACT

In this study, we performed the self-assembly of the amylose-grafted carboxymethyl cellulose sodium salt (NaCMC) for the formation of nanofiber films under aqueous conditions. The introduction of amylose graft chains was conducted by the chemoenzymatic approach including phosphorylase-catalyzed enzymatic polymerization. The product had the rigid NaCMC main chain, which further assembled leading to nanofibers by the formation of double helix between the long amylose graft chains in the intermolecular NaCMC chains of the products. The lengths of the fibers were depended on degrees of polymerization of amylose chains. The nanofiber films were constructed by drying the alkaline solutions of the amylose-grafted NaCMC. The lengths of the nanofibers strongly affected their arrangements in the films. The nanofibers were merged further by washing out alkali to produce the robust nanofiber films.

1. Introduction

Natural polysaccharides are the most abundant organic substances on the earth (Berg, Tymoczko, & Stryer, 2006). Cellulose is a representative polysaccharide and the structure of which consists of a chain of β-(1 → 4)-linked glucose residues (Schuerch, 1986). It is a very important renewable resource that has a number of traditional applications including its use in furniture, clothing, and medical products (Klemm, Heublein, Fink, & Bohn, 2005). Various derivatives of cellulose have also been synthesized and used in practical applications (Doelker, 1993). Carboxymethyl cellulose (CMC), an anionic water-soluble polysaccharide, is one of the most widely applied cellulose derivatives, which can be used in various fields such as detergent, food, paper, and textile industries (Stephen, Philips, & Williams, 1995). A sodium salt of CMC (NaCMC) has a number of sodium carboxymethyl groups ($-CH_2CO_2Na$), which promote water solubility. NaCMC has facile film formability although the film is water-soluble or swellable. Besides linear polysaccharides such as cellulose, branched hetero structures have often been observed in natural polysaccharides, where a polysaccharide of the main chain accompanies different kinds of branched saccharide chains by covalent linkages (Schuerch, 1986). The development of efficient methods for the preparation of branched or grafted artificial heteropolysaccharides using common polysaccharides, therefore, is a promising topic in bio-based material research fields.

In this paper, we report the self-assembly of a new NaCMC-based heteropolysaccharide, which has the graft chains of another natural glucose polymer linked through α-(1 → 4)-glycosidic linkages, that is, amylose (Berg et al., 2006; Schuerch, 1986), successfully giving rise to nanofiber films. For the synthesis of the material, i.e., an amylose-grafted NaCMC, we employed chemoenzymatic technique combined of phosphorylase-catalyzed enzymatic polymerization forming amylose with chemical reaction, which was recently developed by us (Kaneko & Kadokawa, 2009; Omagari & Kadokawa, 2011). The enzymatic polymerization by the phosphorylase catalysis is performed using α-D-glucose 1-phosphate (G-1-P) as a monomer (Fujii et al., 2003; Kitaoka & Hayashi, 2002; Ohdan, Fujii, Yanase, Takaha, & Kuriki, 2006; Yanase, Takaha, & Kuriki, 2006; Ziegast & Pfannemüller, 1987). To initiate the polymerization, a maltooligosaccharide as a primer is necessary. The propagation proceeds through the following reversible reaction to produce amylose; $(\alpha\text{-}(1 \rightarrow 4)\text{-G})_n + \text{G-1-P} \leftrightarrows (\alpha\text{-}(1 \rightarrow 4)\text{-G})_{n+1} + \text{P}$. The degrees of polymerization (DPs) of the produced amyloses were controlled by the feed molar ratios of G-1-P/primer. For the synthesis of the amylose-grafted heteropolysaccharides in the previous investigations, the maltooligosaccharide primers were first introduced on the main chain polysaccharides by chemical reactions, and then, the phosphorylase-catalyzed enzymatic polymerization from the primers were conducted. By means of the chemoenzymatic technique, we have previously reported the synthesis of amylose-grafted chitin/chitosan, cellulose, alginate, and xanthan gum (Arimura, Omagari, Yamamoto, & Kadokawa, 2011; Kaneko, Matsuda, & Kadokawa, 2007; Matsuda, Kaneko, & Kadokawa, 2007; Omagari, Matsuda, Kaneko, & Kadokawa, 2009; Omagari, Kaneko, & Kadokawa, 2010). The resulting materials often

---

* Corresponding author. Tel.: +81 99 285 7743; fax: +81 99 285 3253.
E-mail address: kadokawa@eng.kagoshima-u.ac.jp (J.-i. Kadokawa).

0144-8617/$ – see front matter © 2012 Elsevier Ltd. All rights reserved.
http://dx.doi.org/10.1016/j.carbpol.2012.07.006

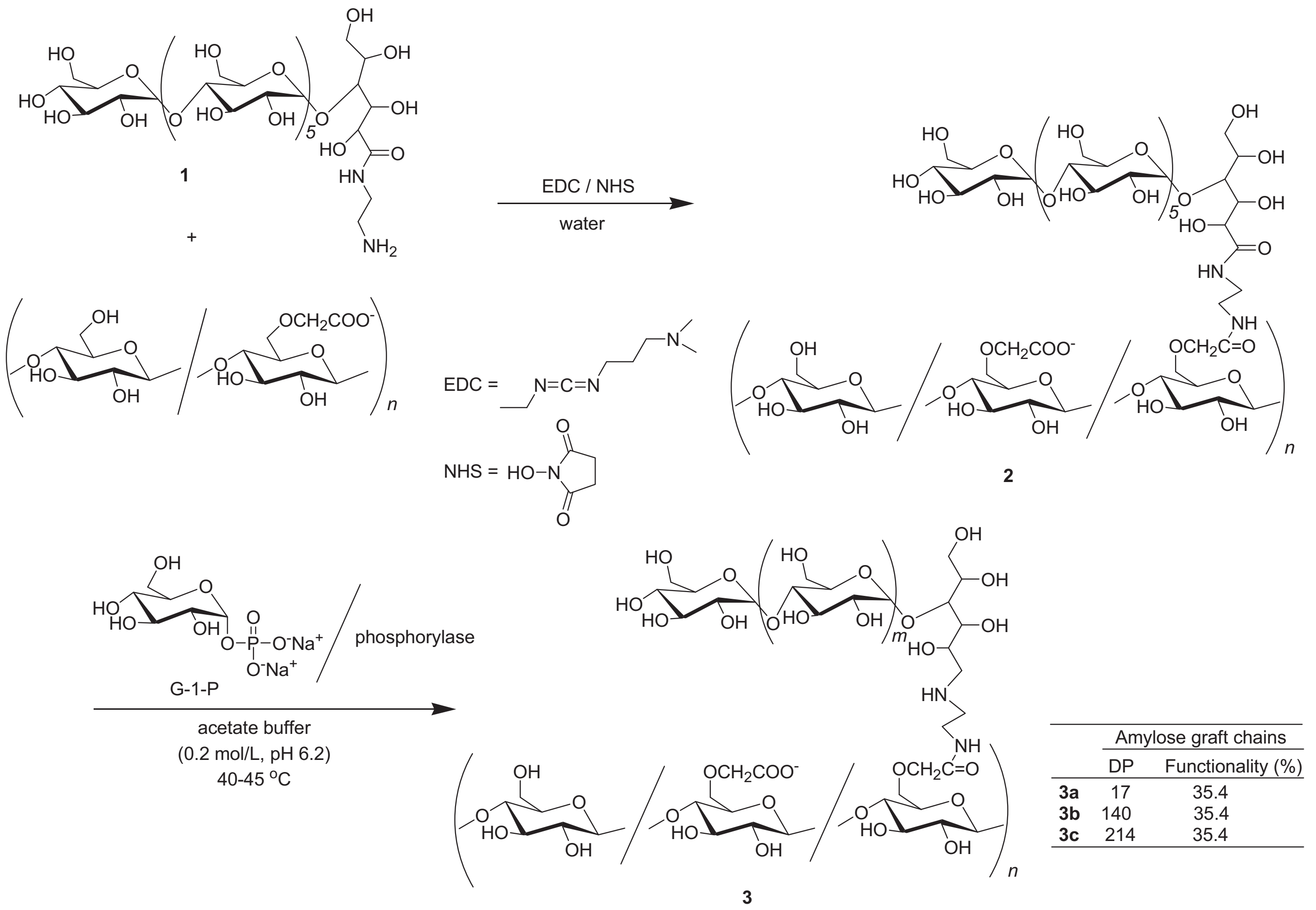

	Amylose graft chains	
	DP	Functionality (%)
3a	17	35.4
3b	140	35.4
3c	214	35.4

Scheme 1. Chemoenzymatic synthesis of amylose-grafted NaCMC (**3**).

exhibited different properties and natures from those of amylose and the main chain polysaccharides.

In this study, we synthesized the desired amylose-grafted NaCMCs with different functionalities and DP of the graft chains by means of the above chemoenzymatic technique (Scheme 1). Then, self-assembling property of the products under aqueous conditions was evaluated by the SEM measurement, which showed the formation of nanofibers. From the materials with longer amylose graft chains, furthermore, robust films were obtained by the formation of long nanofibers from their alkaline solutions and subsequent cross-linking process through double-helix formation between the amylose graft-chains in fibers by washing out alkali. Self-assembled fibrillar nanostructures from biological macromolecules such as cellulose are promising materials for the practical applications in bio-related research fields such as tissue engineering (Abdul Khalil, Bhat, & Ireana Yusra, 2012; Beglou & Haghi, 2008; Isogai, Saito, & Fukuzumi, 2011). Conventional approaches to the production of cellulose nanofibers are mainly performed upon top-down procedures that break down the starting bulk materials from natural resources. For example, the cellulose nanofibers were produced through disintegration process from native cellulose by TEMPO-mediated oxidation or mechanical treatment (Abe, Iwamoto, & Yano, 2007; Saito, Kimura, Nishiyama, & Isogai, 2007; Saito, Nishiyama, Putaux, Vignon, & Isogai, 2006). The present method reported herein is the completely different approach from the above to produce nanofibers of cellulose derivative, that accords to self-assembling generative (bottom-up) route, in which fibrillar nanostructures are produced by regeneration from the solutions of cellulosic materials via appropriate process, as an example of the previously reported electrospinning equipment (Ma, Kotaki, & Ramakrishna, 2005). This approach, moreover, provides a new efficient method for cross-linking among nanofibers by the interaction of graft-chains present on them to construct the morphologically controlled materials.

2. Experimental part

2.1. Materials and methods

Commercially available NaCMC (average M_w; ca 250,000, degree of substitution (DS) = 0.7) was purchased from Sigma–Aldrich Chemical Co. Thermostable phosphorylase (from *Aquifex aeolicus* VF5, ca. 180 unit/mL) was supplied from Ezaki Glico Co. Ltd., Osaka, Japan. An amine-functionalized maltooligosaccharide (**1**) was synthesized according to literature procedure reported by us (Omagari et al., 2010). Synthesis of maltooligosaccharide-grafted NaCMC (**2**) was conducted by the reaction of **1** with NaCMC in water using 1-ethyl-3-(3-dimethylaminopropyl)carbodiimide hydrochloride (EDC)/*N*-hydroxysuccinimide (NHS) as a condensing agent (detailed procedure see supplementary data). Other reagents and solvents were used as received. ^{1}H NMR spectra were recorded on a JEOL ECX-400 spectrometer. SEM images were obtained using Hitachi SU-70 electron microscope. XRD measurements were conducted using PANalytical X'Pert Pro MPD with Ni-filtered Cu Kα radiation (λ = 0.15418 nm). The stress–strain curves under tensile mode were measured using a tensile tester (Little Senster LSC-1/30, Tokyo Testing Machine).

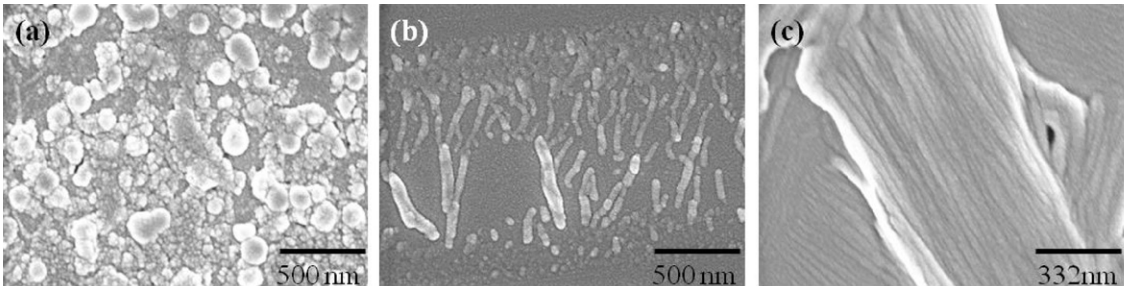

Fig. 1. SEM images of samples NaCMC (a), **2** (b), and **3a** (c) prepared from their aqueous solutions (ca. 1.0×10^{-25} mol/L).

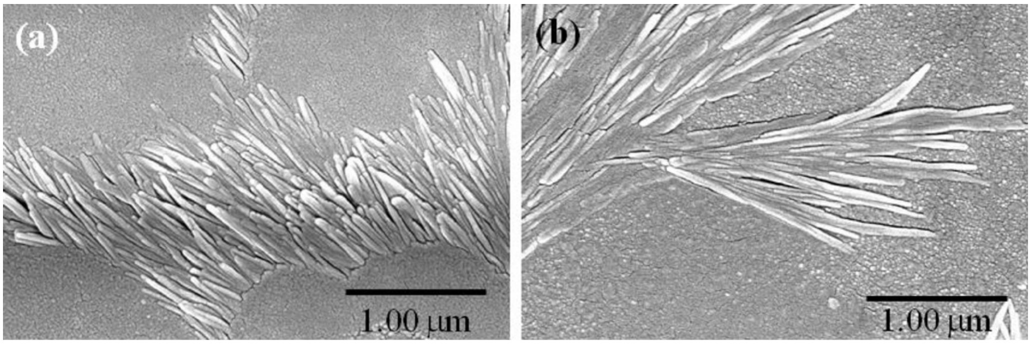

Fig. 2. SEM images of samples **3b** (a) and **3c** (b) prepared from their alkaline solutions (1.0×10^{-4} mol/L).

2.2. *Synthesis of amylose-grafted NaCMC (**3**)*

The aforementioned **2** was dissolved in aqueous acetate buffer (0.2 mol/L, pH 6.2) and sodium salt of G-1-P was added to the solution. After the pH value of the solution was adjusted to 6.2 by addition of 0.20 mol/L aqueous acetic acid, thermostable phosphorylase was added to this solution, and the solution was stirred at 40–45 °C for 20 h. The reaction mixture was subjected to the

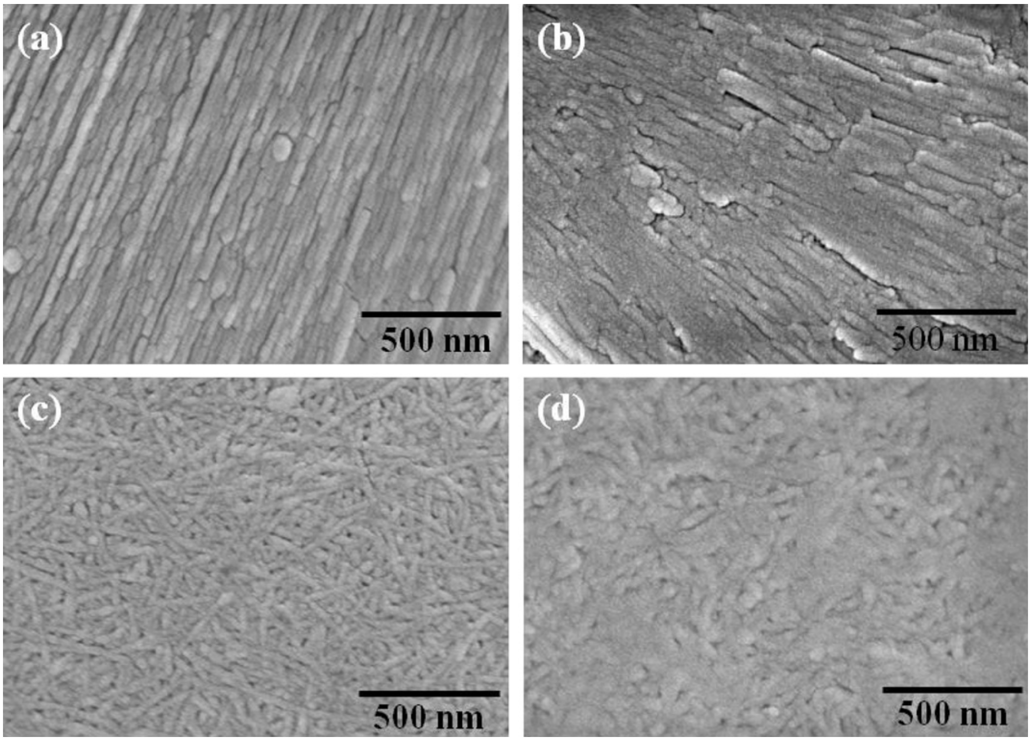

Fig. 3. SEM image of films prepared from alkaline solutions (0.040 g in 0.50 mol/L aqueous NaOH (1.50 mL)) of **3b** and **3c** (a and c, respectively), and films after washing out alkali (b and d, respectively).

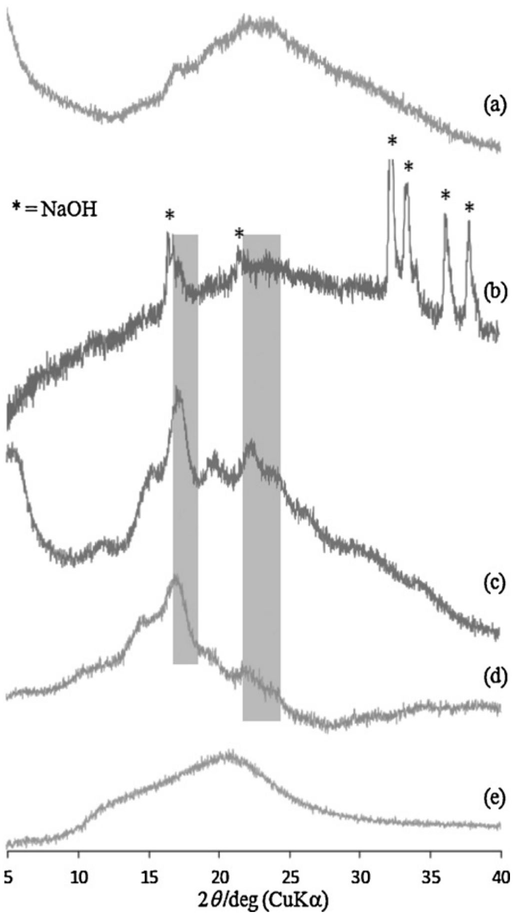

Fig. 4. XRD profiles of films of **3a** (a), of **3c** (b, containing alkali), of **3c** (c, without alkali), amylose (d), and NaCMC (e).

appropriate procedure to give **3**. The detailed preparative procedures for the representative samples of **3** were described in supplementary data.

2.3. *Preparation of film from **3** with graft chains of high DPs*

The powdered sample **3** of run 9 or 10 in Table S1 (0.040 g) was dissolved in 0.50 mol/L aqueous NaOH (1.50 mL) with stirring at room temperature. The alkaline solution was spread thinly on a Petri dish and left standing at room temperature for dryness to give a film containing alkali. The resulting material was immersed in water (10 mL) for 10 min, followed by immersion in water (5 mL) for 5 min to wash out alkali. Then, the material was left standing at room temperature for dryness to give a film excluding alkali.

3. Results and discussion

For the preparation of the amylose-grated NaCMCs by the chemoenzymatic technique, the introduction of maltooligosaccharides on NaCMC chains was first performed by the condensation of the amino group in **1** with the carboxylates in NaCMC (M_w; ca. 250,000, DS = 0.7) using a condensing agent of EDC/NHS in water at room temperature to produce a maltooligosaccharide-grafted NaCMC (**2**) (Scheme 1). The product, which was isolated by dialysis against water, followed by precipitation into methanol, was characterized by the ^{1}H NMR measurement in D_2O (Fig. S1). The ratios of the introduced maltooligosaccharide chains to the glucose units (functionality), which were calculated by the integrated ratios of the α-anomeric signals to β-anomeric signals, were controlled by the feed ratios of **1** to NaCMC in the condensation.

The synthesis of the amylose-grafted NaCMC (**3**) with shorter graft chains was performed by the phosphorylase-catalyzed enzymatic polymerization of G-1-P from non-reducing ends of maltooligosaccharide (primer) graft chains in **2** (functionality of graft chain; 35.4%) in the low feed ratio, that is, G-1-P/primer = 5, in 0.20 mol/L sodium acetate buffer (pH 6.2) at 40–45 °C for 20 h (run 7, Table S1). The product **3a** was isolated by dialysis against water and purified further by precipitation into methanol. The isolated product was soluble in water, and thus, was characterized by the ^{1}H NMR measurement in D_2O (Fig. S2), which showed obvious increase of the integrated ratio of α-anomeric signal to β-anomeric signal compared with that in the ^{1}H NMR spectrum of **2** (Fig. S1). An average DP of amylose graft chains was calculated on the basis of the elemental analysis data of **3a** and the functionality of maltooligosaccharide chain in **2** to be 17.

To evaluate self-assembling property of the resulting material **3a** under aqueous conditions, the SEM measurement was conducted. A diluted aqueous solution (ca. 1.0×10^{-25} mol/L) of **3a** on an aluminum plate was dried under ambient conditions to provide a SEM sample. Fig. 1c shows the SEM image of the sample **3a** in comparison with that of samples NaCMC and **2** (functionality of graft chain; 35.4%) prepared by the same procedure (Fig. 1a and b, respectively). The SEM image of NaCMC showed morphology of uncontrolled particles, whereas rod-like aggregates with 70 and 433 nm in average width and length, respectively, were seen in that of **2**. Furthermore, bundles of some fibrils, where each fiber had an average 39 nm width, were observed in the SEM image of **3a**. These results indicated that **2** and **3a** favorably formed rigid assemblies under aqueous conditions, probably because of the presence of a number of graft chains on the NaCMC chain, which prevented to construct random-coil conformation.

Then, water-insoluble materials of **3** were prepared by introducing the longer amylose graft chains to evaluate the more detailed self-assembling property under aqueous conditions. Accordingly, the phosphorylase-catalyzed polymerization of G-1-P in the higher feed ratios of G-1-P/primer (100, 300, and 500) was carried out using **2** with the different functionalities of maltooligosaccharides (10.0, 21.2, and 35.4) as shown in Table S1. All the products were insoluble in water, but soluble in aqueous alkaline solution, and thus, their structures were confirmed by the ^{1}H NMR measurement in 1.0 mol/L NaOD/D_2O (Fig. S3, run 1, Table S1). In addition to the fact that an aqueous alkaline solution is a good solvent for amylose, the presence of sodium carboxymethyl groups probably contributed to solubilization of the products in the alkaline solution. The average DPs of amylose graft chains were higher than those in the aforementioned **3a** and were controlled by changing the feed ratios of G-1-P/primer.

When the phosphorylase-catalyzed polymerization of G-1-P using **2** was carried out under the conditions of runs 9 and 10, the resulting reaction mixtures turned into gel form. Therefore, the products were isolated by immersing the mixtures in water, followed by lyophilization to give **3b** and **3c** (DP; 140 and 214, respectively, functionality; 35.4%). The SEM measurement of **3b** and **3c** was conducted using their samples prepared by dryness of the diluted alkaline solutions (1.0×10^{-4} mol/L) in 5.0×10^{-4} mol/L aqueous NaOH under ambient conditions. In the SEM images of the samples **3b** and **3c** (Fig. 2a and b, respectively), morphologically controlled nanofibers were clearly seen, indicating that the presence of the long amylose graft chains obviously contributed to the formation of nanofibers. An average length of the fibers from **3c** (1.43 μm) was longer than that from **3b** (0.66 μm) with similar average widths (32.5 and 37.5 nm, respectively), suggesting the lengths of nanofibers were depended on DPs of amylose graft chains on the CMC chains.

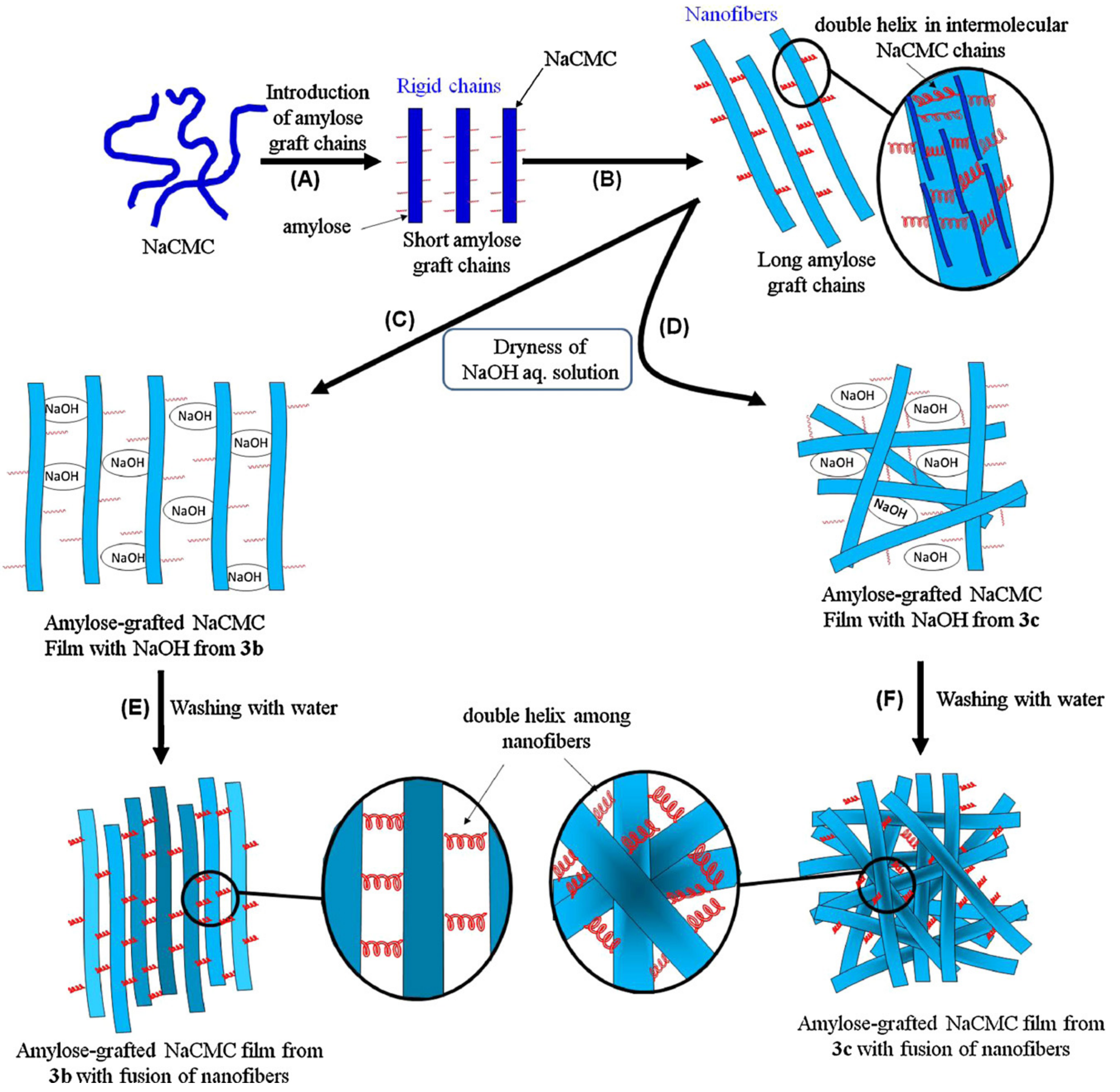

Fig. 5. Proposed self-assembling process of **3** under aqueous conditions leading to nanofiber film.

The films were obtained by dryness of the thinly spread alkaline solutions of **3b** and **3c** in a higher concentration (0.040 g in 0.50 mol/L aqueous NaOH (1.50 mL)); the films still contained alkali. It was confirmed from the SEM image (Fig. 3a) that the film of **3b** was constructed from nanofibers arrayed in parallel. The SEM image (Fig. 3c) showed the film of **3c** was also constructed from nanofibers, but which was arranged in highly condensed entanglement. These results indicated that DPs of graft chains on the CMC chains strongly affected the arrangements of nanofibers in the films. Then, alkali present in the films was removed by immersion in water. The SEM images (Fig. 3b and d) of the resulting films without alkali showed that the nanofibers were merged each other at interfacial area with remaining the fiber arrangements as observed in the films before washing out alkali.

To evaluate the role of amylose graft chains on the construction of the nanofiber films, the powder XRD measurement was conducted. In the XRD profile of the film of **3c** with the long graft chains (DP; 214), corresponding to that of Fig. 3c, diffraction peaks due to amylose double helix, as observed in the XRD profile of a sole amylose (Fig. 4d), were slightly observed (indicated with shadows) besides diffraction peaks due to NaOH (Fig. 4b) (Potocki-Veronese et al., 2005; Putaux, Potocki-Véronèse, Remaud-Simeon, & Buleon, 2006). The diffraction peaks of amylose helix were not significantly appeared in the XRD profile of the film of **3a** with the shorter graft chains (Fig. 4a). These results suggested that the longer amylose graft chains favorably formed double helix in the intermolecular rigid CMC chains to contribute to the construction of the long nanofibers although the formation of amylose double helix was generally prevented in an alkaline solution due to its nature of a good solvent for amylose. After washing out alkali from the film of **3c**, the large diffraction peaks due to amylose double helix were observed as shown in Fig. 4c. This data indicated that the double helix formation among nanofibers occurred by exclusion of alkali from the film, leading to fusion of the fibers. The XRD profiles from **3b** showed the similar results as those from **3c** in Fig. 4b and c. The above XRD results suggested the large influence of the

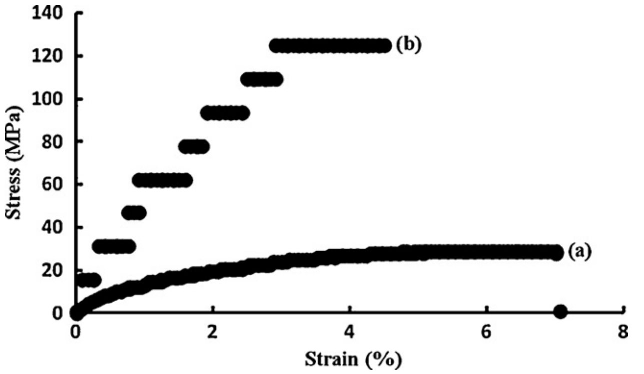

Fig. 6. Stress–strain curves of the films from **3b** (a) and **3c** (b) after washing out alkali.

grafted amylose chain lengths on the efficient formation of the nanofibers. However, the critical chain lengths for the formation of the nanofibers are not yet clear. Because the nanofiber formation is probably affected by the functionality of the amylose graft chain and the chain length of CMC as well, the detailed study on the effects of these factors is now in progress.

On the basis of the above results, we propose the following self-assembling process of **3** under aqueous conditions, leading to the nanofiber film (Fig. 5). Non-crystalline NaCMC chains, which was confirmed by no appearance of significant crystalline peak in the XRD profile (Fig. 4e), form rigid conformation by the introduction of a number of maltooligosaccharide or amylose chains on the NaCMC chains (process **(A)**). Because the short amylose chains, i.e., DP = 17, do not sufficiently form double helix, which was confirmed by the XRD measurement (Fig. 4a), **3a** only constructs a bundle of fibrils. While the longer amylose chains form double helix to assist intermolecular aggregation of the rigid **3c** and **3b** molecules, clearly leading to the nanofiber formation (process **(B)**). During the film formation from **3b** and **3c** under alkaline conditions, the morphologically controlled self-assembly of nanofibers depending on the lengths of fibers occurs, where the shorter nanofibers from **3b** array in parallel (process **(C)**), whereas the longer nanofibers from **3c** are highly entangled (process **(D)**). By washing out alkali from the films, the double helix formation between amylose chains on the nanofibers are progressed, leading to fusion of the fibers (processes **(E)** and **(F)**).

Finally, mechanical properties of the films of **3b** and **3c** after washing out alkali were evaluated by tensile testing. The stress–strain curves of both the films under tensile mode (Fig. 6) showed the large fracture stress values, indicating their robust natures. The film of **3b** showed more elastic nature, which was elongated to the 6.9% fracture strain with the 29 MPa fracture stress. While harder nature was significantly confirmed in the film of **3c** by appearance of the much higher fracture stress (125 MPa) and the lower fracture strain (4.5%). These results suggested that the arrangements of nanofibers in the films strongly affected mechanical properties.

4. Conclusions

In this paper, we reported the morphologically controlled self-assembly of the amylose-grafted NaCMC **3** for the formation of the nanofiber films under aqueous conditions. The introduction of amylose graft chains contributed to the construction of the rigid NaCMC main chain. The long amylose graft chains formed double helix in the intermolecular NaCMC chains of **3** to give nanofibers with the different lengths depending on DPs of amylose chains. The nanofiber films were constructed by dryness of the alkaline solutions of **3**, where arrangements of the fibers were depended on DPs of amylose chains. The nanofibers were merged further by washing out alkali to produce the water-insoluble and robust nanofiber films of **3**. Such water-insolubility and highly strength of the resulting films were superiorly different from the sole NaCMC and amylose, respectively, and accordingly, are useful properties as the materials for new applications. The present study provides the morphologically controlled self-assembly of heteropolysaccharides to produce new nanofibrillar materials. The resulting nanofiber films are considered to be bio-compatible and eco-friendly materials because of consisting of natural polysaccharide resources. We, therefore, will investigate practical applications of the present materials in medical, pharmaceutical, tissue materials, and the related research fields.

Acknowledgment

A donation of phosphorylase by Ezaki Glico Co. Ltd., Osaka, Japan, is gratefully acknowledged.

Appendix A. Supplementary data

Supplementary data associated with this article can be found, in the online version, at http://dx.doi.org/10.1016/j.carbpol.2012.07.006.

References

Abdul Khalil, H. P. S., Bhat, A. H., & Ireana Yusra, A. F. (2012). Green composites from sustainable cellulose nanofibrils: A review. *Carbohydrate Polymers*, *87*, 963–979.

Abe, K., Iwamoto, S., & Yano, H. (2007). Obtaining cellulose nanofibers with a uniform width of 15 nm from wood. *Biomacromolecules*, *8*, 3276–3278.

Arimura, T., Omagari, Y., Yamamoto, K., & Kadokawa, J. (2011). Chemoenzymatic synthesis and hydrogelation of amylose-grafted xanthan gums. *Carbohydrate Polymers*, *49*, 498–503.

Beglou, M. J., & Haghi, A. K. (2008). Electrospun biodegdadable and biocompatible natural nanofibers: A detailed review. *Cellulose Chemistry and Technology*, *42*, 441–462.

Berg, J. M., Tymoczko, J. L., & Stryer, L. (2006). *Biochemistry* (6th International edition). New York: W.H. Freeman & Co. (Chapter 11)

Doelker, E. (1993). Cellulose derivatives. *Advances in Polymer Science*, *107*, 199–265.

Fujii, K., Takata, H., Yanase, M., Terada, Y., Ohdan, K., Takaha, T., et al. (2003). Bioengineering and application of novel glucose polymers. *Biocatalysis and Biotransformation*, *21*, 167–172.

Isogai, A., Saito, T., & Fukuzumi, H. (2011). TEMPO-oxidized cellulose nanofibers. *Nanoscale*, *3*, 71–85.

Kaneko, Y., & Kadokawa, J. (2009). Chemoenzymatic synthesis of amylose-grafted polymers. In R. Ito, & Y. Matsuo (Eds.), *Handbook of carbohydrate polymers: Development, properties and applications* (pp. 671–691). Hauppauge: Nova Science Publishers, Inc (Chapter 23).

Kaneko, Y., Matsuda, S., & Kadokawa, J. (2007). Chemoenzymatic syntheses of amylose-grafted chitin and chitosan. *Biomacromolecules*, *8*, 3959–3964.

Kitaoka, M., & Hayashi, K. (2002). Carbohydrate-processing phosphorolytic enzymes. *Trends in Glycoscience and Glycotechnology*, *14*, 35–50.

Klemm, D., Heublein, B., Fink, H. –P., & Bohn, A. (2005). Cellulose: Fascinating biopolymers and sustainable raw material. *Angewandte Chemie (International ed.)*, *44*, 3358–3393.

Ma, Z., Kotaki, M., & Ramakrishna, S. (2005). Electrospun cellulose nanofiber as affinity membrane. *Journal of Membrane Science*, *265*, 115–123.

Matsuda, S., Kaneko, Y., & Kadokawa, J. (2007). Chemoenzymatic synthesis of amylose-grafted chitosan. *Macromolecular Rapid Communications*, *28*, 863–867.

Ohdan, K., Fujii, K., Yanase, M., Takaha, T., & Kuriki, T. (2006). Enzymatic synthesis of amylose. *Biocatalysis and Biotransformation*, *24*, 77–81.

Omagari, Y., & Kadokawa, J. (2011). Synthesis of heteropolysaccharides having amylose chains using phosphorylase-catalyzed enzymatic polymerization. *Kobunshi Ronbunshu*, *68*, 242–249.

Omagari, Y., Kaneko, Y., & Kadokawa, J. (2010). Chemoenzymatic synthesis of amylose-grafted alginate and its formation of enzymatic disintegratable beads. *Carbohydrate Polymers*, *82*, 394–400.

Omagari, Y., Matsuda, S., Kaneko, Y., & Kadokawa, J. (2009). Chemoenzymatic synthesis of amylose-grafted cellulose. *Macromolecular Bioscience*, *9*, 450–455.

Potocki-Veronese, G., Putaux, J.-L., Dupeyre, D., Albenne, C., Remaud-Siméon, M., Monsan, P., et al. (2005). Amylose synthesized in vitro by amylosucrase: Morphology, structure, and properties. *Biomacromolecules*, *6*, 1000–1011.

Putaux, J.-L., Potocki-Véronèse, G., Remaud-Simeon, M., & Buleon, A. (2006). α-D-Glucan-based dendritic nanoparticles prepared by in vitro enzymatic chain extension of glycogen. *Biomacromolecules*, *7*, 1720–1728.

Saito, T., Kimura, S., Nishiyama, Y., & Isogai, A. (2007). Cellulose nanofibers prepared by TEMPO-mediated oxidation of native cellulose. *Biomacromolecules*, *8*, 2485–2491.

Saito, T., Nishiyama, Y., Putaux, J. L., Vignon, M., & Isogai, A. (2006). Homogeneous suspensions of individualized microfibrils from TEMPO-catalyzed oxidation of native cellulose. *Biomacromolecules*, *7*, 1687–1691.

Schuerch, C. (1986). Polysaccharides. In H. F. Mark, N. Bilkales, & C. G. Overberger (Eds.), *Encyclopedia of polymer science and engineering* (2nd edition, 13, pp. 87–162). New York: John Wiley & Sons.

Stephen, A. M., Philips, G. O., & Williams, P. A. (1995). *Food polysaccharides and their applications*. London: Taylor & Francis.

Yanase, M., Takaha, T., & Kuriki, T. (2006). α-Glucan phosphorylase and its use in carbohydrate engineering. *Journal of the Science of Food and Agriculture*, *86*, 1631–1635.

Ziegast, G., & Pfannemüller, B. (1987). Phosphorolytic syntheses with di-, oligo- and multi-functional primers. *Carbohydrate Research*, *160*, 185–204.